Mössbuaer relaxation studies of non-linear dynamical excitations in low-dimensional magnets

Groot, H.J.M. de; Jongh, L.J. de; Elmassalami, M.; Smit, H.H.A.; Thiel, R.C.

Hyperfine Interactions 27 (1986) 93-110

MÖSSBAUER RELAXATION STUDIES OF NON-LINEAR DYNAMICAL EXCITATIONS IN LOW-DIMENSIONAL MAGNETS

H.J.M. DE GROOT, L.J. DE JONGH, M. ELMASSALAMI,

H.H.A. SMIT and R.C. THIEL

Kamerlingh Onnes Laboratorium der Rijksuniversiteit Leiden, Nieuwsteeg 18, 2311 SB Leiden, Nederland

Mössbauer effect spectroscopy provides an excellent probe to study domain wall dynamics in the quasi 1-d Ising-type magnetic chain. Theoretical aspects of moving domain walls (nonlinear excitations, kinks, solitons) are briefly discussed, both for quantum and classical 1-d systems. We review experimental data on $Fe(N_2H_5)_2(SO_4)_2$, $RbFeCl_3.2H_2O$ and $FeCl_2(NC_5H_5)_2$. Analysis of the spectra is performed in two different ways: by extracting linewidths, and by fitting to the Blume-Tjon relaxation model, which is argued to give the exact description for the Mössbauer spectrum of a magnetic chain, subject to free-kink behaviour. Differences between this theory and experiments are discussed.

1. INTRODUCTION

In a number of previous papers /1-4/ we have shown that the dynamics of domain walls (kinks, solitons) and other nonlinear excitations in magnetic chains may be conveniently studied by means of the Mössbauer effect (ME). Domain walls are highly localized excitations, corresponding to transition-regions between two different but energetically degenerate ground states. In a ferromagnet such walls connect neighbouring spin-up and spin-down regions, whereas in an antiferromagnet they form the liaison between the two ground state-configurations obtained by interchange of the two sublattices (cf. fig.1).

Evidently, the passage of a kink at a given site flips the electronic spin of the atom. If the atom has a Mössbauer nucleus the hyperfine field $\vec{B}_{hf}$ will likewise be reversed, so that the flip rate may be probed, provided that it is within the frequency window of the Mössbauer effect (0.1 MHz - 5.10^2 MHz for ^{57}Fe). Flips of the electronic spins are of course also observed by ME due to other types of relaxation effects as e.g. (super-)paramagnetic relaxation /6/. However, the physics behind it is much richer, and consequently it can easily be identified and separated from the other effects, as will be discussed below.

Perhaps superfluously, we remark that nonlinear phenomena are by no means restricted to magnetism. During the last few years they have become increasingly more important in many different fields, notably in the various branches of solid state physics and chemistry. They occur in ferro- and antiferromagnetics /5/, structural transitions /7/, commensurate-incommensurate problems /8/, hydrogen-bonded structures /9/, polymeric chains /10/, spin- and charge-density-wave systems /11,12/, etc., etc. In general one may expect a dynamical behaviour to be associated with these walls. In truly one-dimensional systems they can move freely, whereas in higher dimensions walls tend to be pinned by lattice defects, magnetostatic effects, etc. Nevertheless, dynamic effects on a smaller scale may still occur, due e.g. to meandering of the walls /13/. In certain cases these effects are al-

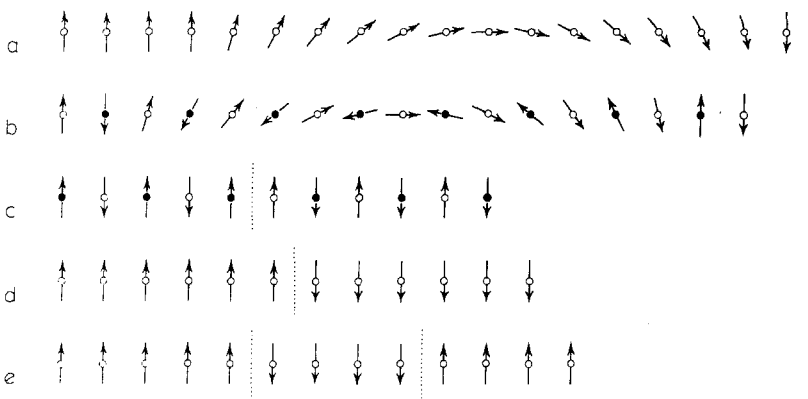

Fig. 1. Non-linear excitations in magnetic chains.
a,b Topological excitation (π-soliton) in a classical ferro- and antiferromagnetic chain.
c,d Topological excitation (domain wall) in the $S=\frac{1}{2}$ antiferro- and ferromagnetic Ising chain.
e Wall-pair excitation in a ferromagnetic $S=\frac{1}{2}$ Ising chain (this excitation is topologically equivalent to the ground-state).

most negligible, as for the ordered 3-d ferromagnet, where, except for a small critical region ($\Delta T/T_c \simeq 0.01$) around the phase transition the wall-pattern appears to be static. On the other hand, in disordered or random 3-d and 2-d systems, wall-dynamics (or cluster-dynamics) is again possible /14/ over wide temperature ranges above the freezing temperature, as for example in spin glasses and amorphous magnets. It is our conviction that the Mössbauer effect presents an excellent probe for the study of these other nonlinear problems as well, so that the ideas developed in the course of magnetic domain-wall studies in quasi 1-d systems may actually have a much wider applicability.

The outline of this brief review is as follows. In the next section some experimental details of the investigated samples are summarized. In sections 3 and 4 the relevant theoretical concepts on the domain wall behaviour are given. An illustrative example of the observed line-broadening is presented in section 5. Thereupon the more extensive methods of analysis of the Mössbauer spectra are outlined in section 6, and are applied to the other experimental results in the last section.

2. DETAILS OF THE INVESTIGATED COMPOUNDS

In the course of a systematic investigation of nonlinear effects we have studied several quasi 1-d magnets with Ising-type anisotropy. In the present section we briefly discuss the magnetic properties of the compounds, which are listed in table I. All are high-spin Fe^{2+} compounds, for which the strong magnetic anisotropies are due to crystal field effects.

The compound $RbFeCl_3.2H_2O$ is a quasi 1-d Ising **antiferromagnet** with effective spin $S = \frac{1}{2}$. In this case the Fe^{2+} ion has a doublet electronic ground state, the other levels being at least 60 K higher in energy /15/. Therefore, the low-temperature magnetic properties are well described by the hamiltonian

$$\mathcal{H} = -2J_x \sum_{i=1}^{N-1} [S_i^x S_{i+1}^x + \varepsilon(S_i^y S_{i+1}^y + S_i^z S_{i+1}^z)] \quad , \qquad (1)$$

Table I
Anisotropy and exchange constants together with calculated and experimental values for the soliton energies for the various compounds.

compound	eff. spin S	J/k_B (K)	D_z/k_B (K)	D_x/k_B (K)	E_s^{calc} (K)	E_s^{exp} (K)
$RbFeCl_3.2H_2O$	½	-39	-	-	39	115±5 (B=0T) 105±5 (B=1.5T)
$FeCl_2(NC_5H_5)_2$	1	3.3	10.5	9.2	22	60 ± 5
	½	25	-	-	25	
$Fe(N_2H_5)_2(SO_4)_2$	2	-2.0	5.6	0.8	20.2	44 ± 5

with intrachain exchange constant $J_x < 0$ and $\varepsilon = \frac{1}{2}(J_y + J_z)/J_x$. The magnetic coupling between the chains is two orders of magnitude smaller than J_x. The value of J_x was obtained by Kopinga et al. /16/, from an analysis of the specific heat. An accurate value for ε is not known, but an upper limit can be estimated from the anisotropy in the g-factor, since $\varepsilon \approx (g_\perp/g_\parallel)^2$. From the behaviour of the magnetic susceptibility (χ) /15/ it was found that $g_x = g_\parallel = 9.6$ and $g_{y,z} = g_\perp \approx 0.5$. Thus the anisotropy is strong ($\varepsilon \approx 0.2$) and almost uniaxial ($J_y \approx J_z$), with the x-axis as the easy axis.

The second compound, $FeCl_2(NC_5H_5)_2$ is an approximation of the Ising-type **ferromagnetic** chain /17/. In an earlier short note /2/ we have already presented χ-data for this system, and in a phenomenological approach we compared these with the prediction for the ferromagnetic S = ½ Ising chain, i.e. eq.(1) with $J_x > 0$ and $\varepsilon = 0$. Good agreement was obtained with $J_x/k_B = 25$ K. Meanwhile we have studied the crystal-field symmetry in more detail, through its effects on the Mössbauer and the optical /18/ spectra. It appears that the total splitting of the lowest quintuplet of the (L=2, S=2) Fe^{2+} ion amounts to 130 K. It can be divided into a doublet and a triplet, the latter being lowest in energy. The splitting of the triplet is 20 K. Therefore the lowest three levels determine the low-temperature properties and it is appropriate to take up a description in terms of an effective spin S = 1. The hamiltonian for the magnetic chain can be written as the sum of an isotropic Heisenberg interaction plus orthorhombic anisotropy terms.

$$\mathcal{H} = \sum_i [-2J \vec{S}_i \vec{S}_{i+1} - D_x (S_i^x)^2 + D_z (S_i^z)^2] \quad . \qquad (2)$$

The anisotropy constants D_x, D_z are given in table I and were chosen so that they reproduce the splitting of the lowest three levels for S = 1. The value of the exchange-constant J/k_B = 3.3 K was deduced from the high-temperature tail of the χ-curve, which was fitted to the Curie-Weiss expression $\chi = C/(T-\theta)$. This yields an estimate for the exchange-parameter, since $J/k_B \approx \frac{3}{4}\,\theta/S(S+1)$ for the quasi 1-d magnet.

The third system, $Fe(N_2H_5)_2(SO_4)_2$ is an S = 2 **antiferromagnetic** chain and can also be described by a Hamiltonian of the form (2), with J < 0. Values for J/k_B and the easy-plane anisotropy D_z were obtained by Witteveen et al. /19/. We estimated the strength of the Ising-anisotropy D_x from the value of the in-plane "spinflop" field /19/ $B_{sf} \approx 7.5$ T with the relation $D_x = g^2\mu_B^2 B_{sf}^2/16|J|S^2$. We have also recalculated the low-temperature crystal-field properties /20/ for this compound, and the results support the S = 2 picture, since the overall splitting of the levels in the lowest quintuplet amounts to 25 K. Also the magnitude of the easy-plane anisotropy D_z is in agreement with the crystal-field calculations. As regards the easy-axis anisotropy D_x, its magnitude is too small to be determined from the Mössbauer data because after subtraction of the lattice contribution one has $\eta V_{zz} \approx 0$.

3. KINKS IN MAGNETIC CHAINS

Theoretically it has been known for some time already /21/ that the motion of domain walls in anisotropic ferromagnets (see fig. 1) should obey the sine-Gordon equation, so that they can be considered as soliton-type excitations. They are highly stable, localized excitations, and should be able to propagate along the chains as long as the interaction is not of the pure Ising-type. More recently it was shown that the same type of excitations can be expected in antiferromagnetic chains as well /22,23/.

In the experimental examples given in the present work, the anisotropy is very strong. To treat such anisotropic cases two possible routes present themselves. First, one may describe the Ising-type chain by a classical Heisenberg hamiltonian (2) with a uniaxial or orthorhombic anisotropy-term. Second, one may consider a strong exchange anisotropy in a quantum-mechanical interaction hamiltonian (1). Both cases will be discussed below. In the first treatment, one starts with the hamiltonian for classical spin vectors $\vec{S}_i$, as given by eq.(2), with J > 0 for the ferromagnetic and J < 0 for the antiferromagnetic chain. If we choose $D_x, D_z > 0$ it follows that the total energy in the system is lowest when the spins are along the x-axis, the z- and y-direction corresponding to the hard and the intermediate axis respectively. Also for orthorhombic symmetry the anisotropy can be considered as effectively Ising. As seen in fig. 1 for both the ferro- and antiferromagnetic domain wall, the moments rotate through an angle π over the wall-width. If the wall is N spins wide, the energy may be estimated as the sum of exchange- and anisotropy terms /24/, yielding

$$E_s \approx \pi^2 |J| S^2/N + N D_x S^2 \quad . \tag{3}$$

The wall-energy and wall-width $d_s = a_o N$ (a_o the lattice-constant) may be obtained by minimizing E_s with respect to N, and one finds $E_s \propto \sqrt{|D_x J|}$ and $N \propto \sqrt{|J/D_x|}$. The domain wall is indeed localized, and has finite width due to the fact that the two terms in eq.(3) compete. Such a competition between two energy-terms is a general property of kink-bearing systems. Since systems with two (or more) competing energy-terms are quite abundant in nature, this explains at

Table II
Relations between the parameters in the anisotropic Heisenberg hamiltonian (3) and the sine-Gordon hamiltonian (4) for the ferromagnetic ($J > 0$) and the antiferromagnetic ($J < 0$) case.

	E_o	m^2	c_o	$E_s = 8mE_o$
$J > 0$	$\frac{1}{2} JS^2$	D_x/J	$2\sqrt{D_z J}\, S$	$4S^2 \sqrt{D_x J}$
$J < 0$	$\frac{1}{2}\lvert J\rvert S^2$	$D_x/\lvert J\rvert$	$4\lvert J\rvert S$	$4S^2 \sqrt{\lvert D_x J\rvert}$

the same time the succes of the domain wall concept in describing physical phenomena.

As regards the magnetic chain hamiltonian (2) with $J < 0$ it has been shown /22/ that in the continuum limit this reduces to the classical sine-Gordon (SG) hamiltonian

$$\mathcal{H}^{SG} = 4E_o \int_{-\infty}^{\infty} \frac{\partial\xi}{2}\left[\left(\frac{\partial\phi}{\partial\xi}\right)^2 + \frac{1}{c_o^2}\left(\frac{\partial\phi}{\partial t}\right)^2 - \frac{m^2}{2}\cos 2\phi\right] \quad . \tag{4}$$

This hamiltonian has been completely solved, and it is known that three types of excitations may occur: spin waves, solitons and anti-solitons (kinks), and breathers /25/. The kink-excitations are extremely stable, since they are not conserved by the normal conservation laws for energy and momentum, but are topologically inequivalent to the ground state. The relations between the parameters in hamiltonians (4) and (2) are given in table II. In eq.(4) E_o determines the energy-scale, ξ denotes the position on the chain and is measured in lattice units, and the field $\phi(\xi)$ corresponds to the angle of the moments with the x-axis. The maximum (cutoff) velocity of the kink is given by c_o and the mass m is the inverse of the width d_s of the kink.

It is important to note that for the antiferromagnet the SG parameters do not depend on D_z, i.e. the uniaxial Ising anisotropy D_x which breaks the symmetry is already sufficient to allow propagation of kinks. This is not so for the ferromagnetic case. There the transformation from (2) to (4) in the continuum limit is more complex and is in fact only possible for $D_z >> D_x$. However, it was shown recently /26,27/ that even when this condition is not fulfilled, topologically stable kinks occur, where the energy of such a kink is well approximated by the prediction from the SG theory: $E_s = 4S^2 \sqrt{\lvert D_x J\rvert}$. The difference comes in the maximum velocity c_o that depends on the anisotropy ratio via the relation $c_o = 2\sqrt{\lvert D_x J\rvert}\, S\left[\left(1+D_z/D_x\right)^{\frac{1}{2}}-1\right]$. It follows that when the easy plane anisotropy is absent ($D_z = 0$), the kinks are static ($c_o = 0$), whereas in the SG limit ($D_z >> D_x$) one obtains $c_o = 2\sqrt{\lvert D_z J\rvert}\, S$. Thus the orthorhombicity of the anisotropy is a necessary prerequisite for the dynamics of **ferromagnetic** kinks, whereas for **antiferromagnetic** kinks a uniaxial symmetry is sufficient to yield propagation (with cutoff velocity $c_o = 4\lvert J\rvert S$).

In actual experimental examples the anisotropy can be very strong, as is the case for $RbFeCl_3.2H_2O$ (see section 2 and table I). From the expression $d_s \propto \sqrt{\lvert J/D_x\rvert}$ it is clear that for strong anisotropy the wall-width may ultimately become less than one lattice unit. Obviously in this limit the classical SG description based upon the continuum limit (wide walls) cannot be applied. One has to take

recourse to another formalism, and this brings us to the second approach, namely the quantum analogue hamiltonian (1), with strong exchange anisotropy, where the spin-components are now quantum-mechanical operators (and $S = \frac{1}{2}$). It was first noted by Villain /23/ that also in this case walls do exist and may exhibit dynamical behaviour, although the physical picture differs somewhat from the SG interpretation in the above. There the kinks may be considered as free particles that obey usual free-gas statistics. In the $S = \frac{1}{2}$ Ising-type chain with small transverse exchange ($\varepsilon \ll 1$), on the other hand, they should rather be considered as tightly bound to a given site i, with a hopping probability towards the sites $i\pm2$. As argued by Ishimura and Shiba /28/, the hamiltonian (1) can be reduced to the 1-d tight-binding model for electrons. In this formalism a soliton-band appears, where different states correspond to walls with different momentum k. For the **antiferromagnet** /23/ (all $J < 0$) the wall-energy is expressed as

$$E_s(k) = |J_x| (1 + 2 \varepsilon \cos 2k) \quad . \tag{5}$$

For the **ferromagnet** /29/ ($J_x > 0$) the situation is again different, and it can be shown that the wall-energy then equals

$$E(k) = |J_x| [1 - \tfrac{1}{2} \varepsilon^2 + 2\delta \cos 2k] \quad . \tag{6}$$

We obtained eq.(6) by applying the Villain model to the $S = \frac{1}{2}$ Ising-type ferromagnetic chain with orthorhombic exchange-anisotropy, where $\delta = \frac{1}{2}(J_y - J_z)/J_x$. If one wishes to associate the band-structure with particle-type motion, this can easily be achieved by defining the velocity as $v(k) = \partial E(k)/\partial k$ for both cases. As in the classical case it follows for the antiferromagnet that kink motion is already possible for uniaxial anisotropy, whereas for the ferromagnet the orthorhombic symmetry is crucial, there being no dispersion if $\delta = 0$.

In the continuous SG system the topological conservation is very strict. Therefore single kinks may only enter the chain from the ends, and furthermore it is possible to excite them in pairs in the middle of the chain (cf. fig. 1). The same holds for the 1-d $S = \frac{1}{2}$ system. Nevertheless, kinks will be present at any temperature because of entropy considerations. According to a well-known simple but powerful argument, first formulated by Landau /30/, long-range order in 1-d systems is impossible for $T \neq 0$, due to the formation of domain walls. If the wall-density amounts to n_s, the energy- and entropy-contributions of the walls to the free energy density may be estimated as

$$\Delta f = n_s \left(E_s - T \ln n_s^{-1}\right) \quad , \tag{7}$$

since each wall has a mean free space n_s^{-1}. It follows immediately that for n_s sufficiently low, Δf becomes negative at $T \neq 0$. Thus a certain number of walls will always be present. (In fact walls are present even at $T = 0$, if the effect of quantum fluctuations is taken into account).

At sufficiently low temperatures, the density of kinks will be very low and one may neglect interactions between them. For a system described by the SG hamiltonian, the density is then calculated as

$$n_s^{SG} = \left(\frac{2}{\pi}\right)^{\frac{1}{2}} m_s \left(E_s/k_B T\right)^{\frac{1}{2}} \exp\left(-E_s/k_B T\right) \tag{8}$$

from an ideal kink-gas treatment /31/. The average kink velocity is given by the classical thermal distribution and amounts to $v_s = c_o(E_s/2k_BT)^{-\frac{1}{2}}$. In the discrete S = ½ system the wall-density may be obtained /32/ by calculating the thermal average over the states in the band. This yields

$$n_s^{QM} = e^{-J_x/k_BT} I_o(2\varepsilon J_x/k_BT) \quad , \tag{9}$$

with I_o the modified Bessel-function. In this case the average wall velocity amounts to $v_s=(4k_BT/\hbar\pi)I_o^{-1}(2\varepsilon J_x/k_BT)\sinh(2\varepsilon J_x/k_BT)$.

From the above equations it appears that in both the classical SG and the QM cases the kink-density is exponentially dependent on the kink creation energy E_s. In a Mössbauer experiment one measures this kink-density n_s, since one observes /1,33/ the flip rate $\Gamma_\omega = n_s v_s$ through line broadening (relaxation effects) and narrowing of the observed hyperfine pattern. The ME probe is insensitive to the kink structure, since the passage of a kink at a given site is so rapid (10^{-11} sec) that the ME nucleus experiences it as an instantaneous flip of the hyperfine field B_{hf}, even if the wall-width should be substantial. It is therefore the **wall-statistics** that is studied in the experiments described below.

4. THE INFLUENCE OF KINKS ON THE MOSSBAUER-LINEWIDTH

In principle, all the physics of the static as well as the dynamic properties is contained in the spin-spin correlation functions. As a consequence of the fact that the passage of a wall is very fast compared to characteristic ME times, the perpendicular (to the easy axis) spin-components present over the wall-width (cf. fig. 1a,b) will have no effect on the ME spectrum /1,33/ (in the pure Ising-flip there are no perpendicular components at all). The major effects will be due to the component parallel to the easy axis $\langle S_x(\xi,t)S_x(0,0)\rangle$. At low temperatures, where the kink-densities are so low that the interactions between kinks can be neglected and the dilute free-kink-gas model may be applied to describe the dynamics, this quantity is given /22,32/ to a very good approximation by the expression

$$\langle S_x(\xi,t)S_x(0,0)\rangle = S^2 \exp\left[i\pi\xi\nu - 2n_s(\xi^2 + v_s^2t^2)^{\frac{1}{2}}\right] \quad , \tag{10}$$

where $\nu = 0$ for the ferromagnet and $\nu = 1$ for the antiferromagnet. Since the ME is a local probe, it is the autocorrelation function that is measured. Putting $\xi = 0$ in eq.(9), this function is found to be

$$\langle S_x(t)S_x(0)\rangle = S^2 \exp(-2\Gamma_\omega t) \quad , \tag{11}$$

with $\Gamma_\omega = n_s v_s$ the flip rate. Eqs. (10) and (11) were argued /32/ to be valid both for the classical case as well as for the quantum-case.

The most striking effect in the Mössbauer spectrum is the anomalous increase in the linewidth $\Delta\Gamma$. This excess linewidth is directly related /1/ to the autocorrelation function by the expression $\Delta\Gamma \propto \Gamma_\omega/(2\omega_L^2 + \Gamma_\omega^2)$. The ME is thus sensitive to the kink-process in the temperature region where Γ_ω is comparable to the characteristic time of the ME experiment determined by the nuclear Larmor-frequency $\omega_L \approx 10^7$ s^{-1}. Thus at high temperatures, where the flip rate is very fast compared to ω_L, one has $\Delta\Gamma \propto 1/\Gamma_\omega$. In this region the "exchange-narrowing" of the effective hyperfine field due

to high-frequency fluctuations of the electronic spin is the main mechanism that causes line-broadening. As the temperature is lowered $\Delta\Gamma$ will pass through a maximum near ω_L. Then another physical process takes over, namely nuclear spin relaxation. Finally, for slow fluctuations $\Gamma_\omega \ll \omega_L$ one has $\Delta\Gamma \propto \Gamma_\omega$, so that the broadening will again disappear. Thus the whole line broadening process can be seen as arising from the combination of relaxation due to transitions between different nuclear spin-states induced by the electronic spin-flips and the vanishing of $\vec{B}_{hf}$ at high T when the flip rate becomes very fast.

Since ω_L is of the order of $10^7 s^{-1}$, the ME provides a valuable complementary probe to investigate the wall-dynamics, as compared to quasi-elastic neutron-scattering. There one may probe the full (space-time) fourier-transform of the correlation function, the dynamic structure factor, which is expressed as

$$S_x(k,\omega) = \frac{4\pi n_s S^2}{v_s} \left[q^{*2} + \left(\frac{\omega}{v_s}\right)^2 + \left(2n_s\right)^2 \right]^{-3/2} , \qquad (12)$$

with $q^* = q$ for the ferromagnet and $q^* = q-\pi$ for the antiferromagnet /32/. Eq.(12) describes the shape of the central peak that appears in the neutron diffraction pattern and may be probed by varying both k and ω. However, one is restricted in frequency to 10^9 Hz as a lower limit. Considering that $S_x(k,\omega)$ peaks at $\omega = 0$ with a FWHM $\Delta\omega \simeq 1.53\ \Gamma_\omega$, the lowest values for Γ_ω that may be obtained with good accuracy are of the order of 10^{-2} THz. Therefore only processes that take place on short time-scales ($t < 10^{-10}$ sec) are detected by neutron scattering. The ME, although a local probe, measures orders of magnitude longer (time scales 10^{-9}-10^{-5} s) and thus provides additional information about the dynamics of the kinks close to the maximum of the central peak, given by eq.(12).

5. LINE BROADENING IN $Fe(N_2H_5)_2(SO_4)_2$

As an example we show in fig. 2 some ME spectra taken for $Fe(N_2H_5)_2(SO_4)_2$. At the highest temperatures, only the quadrupole splitting is present and a doublet is observed. As the temperature is lowered, Γ_ω decreases and the effective hyperfine field B_{hf} increases. At 6.3 K (well above T_c = 6.0 K) one already has a fully magnetically split spectrum, but still with very broad lines. At the lowest temperatures measured, the lines are narrow again, since the relaxation is outside the Mössbauer frequency window. The spectra were fitted with a superposition of lorentzian lines, and in fig. 3 we have plotted the linewidth $\Gamma = \Delta\Gamma + \Gamma_o$ versus T^{-1}. In the ideal case Γ_o would be equal to the natural linewidth (0.194 mm/sec for ^{57}Fe). In an experimental system however, there is always some excess linewidth that may be caused by effects such as small vibrations in the equipment. We have taken Γ_o from an experiment on $Fe_xZn_{1-x}(N_2H_5)_2(SO_4)_2$, with x = 0.07. Since Zn^{2+} is nonmagnetic, most of the (magnetic) Fe ions ($\simeq$ 85%) are in a nonmagnetic surrounding. A spectrum was taken at T = 4.2 K (well below T_c = 6.0 K in the pure Fe compound) and indeed a narrow quadrupole doublet was observed. We note that this experiment at the same time definitely excludes the possibility of ascribing the observed broadening to single-ion relaxation effects. The experimental linewidth in this spectrum (Γ = 0.32 mm/sec) was used as rest linewidth Γ_o in the analysis of the spectra taken for the pure compound. From fig. 4 one concludes that $\Delta\Gamma$ increases and decreases exponentially as the temperature decreases, in agreement with the prediction from the kink free-gas theory. The decrease of $\Delta\Gamma$, however, is much sharper below T_c. We interpret this as a blocking of the walls by the 3-d long-range

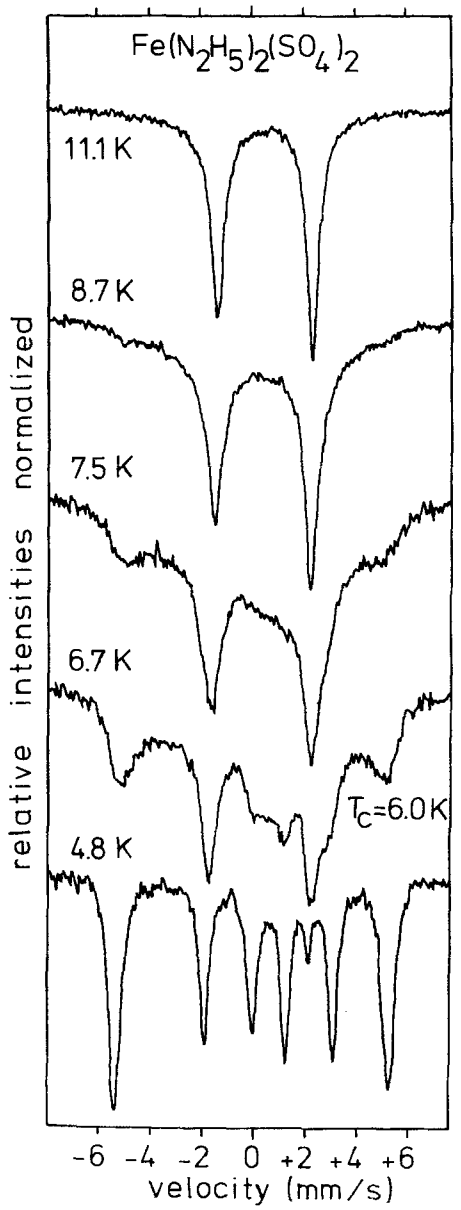

Fig. 2. Some representative Mössbauer transmission spectra taken from $Fe(N_2H_5)_2(SO_4)_2$ at different temperatures.

order, so that the propagation stops and thus the relaxation in the ME disappears.

Also shown in this figure are data for $\Delta\Gamma$ taken from source measurements in ^{57}Co in $Co(N_2H_5)_2(SO_4)_2$. In this compound the linewidth is constant over the whole temperature region, and stays at a low value, although this steady Γ_o is somewhat larger than in the Fe-chain, due to the different and more difficult circumstances in a source-measurement. The reason for this behaviour is that in the Co-chain the anisotropy is of the XY instead of the Ising-type. It was explained in section 3 that the domain walls only occur when the symmetry is broken by an Ising-type component of sufficient strength. Therefore the absence of broadening in the otherwise isostructural

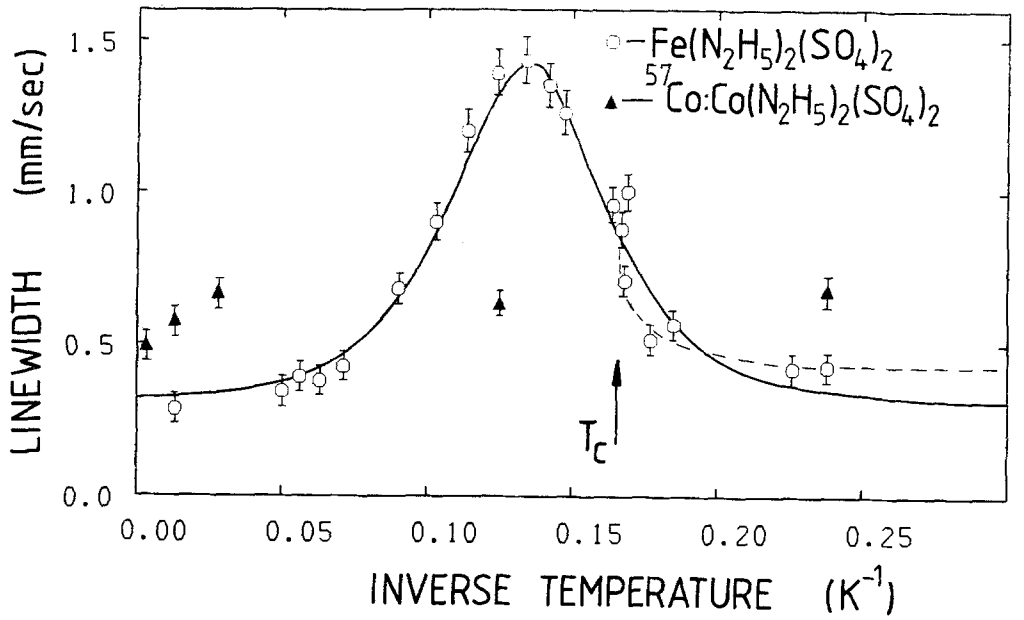

Fig. 3. Linewidth versus inverse temperature for the $Fe(N_2H_5)_2(SO_4)_2$ (o) and $Co(N_2H_5)_2(SO_4)_2$ (Δ) compounds. The spectra were fitted with a superposition of lorentzian lines. The solid line represents the calculated behaviour according to the free-kink gas model, with E_s = 44 K. The residual linewidth (Γ_o) at high temperatures is somewhat less than at low temperatures.

Co-compound provides additional evidence in favour of the kink-model explanation for the broadening in the Fe compound.

The set of experiments discussed in the above yield strong evidence that the relaxation effects are due to collective spin processes in the quasi 1-d Ising system, and also the specific features predicted by the kink free-gas model appear to be nicely reproduced. In practice, however, it is cumbersome (and even questionable) to extract $\Delta\Gamma$ directly from the spectra, and in order to improve the accuracy of the analyses, we have chosen another approach which will be discussed in the next section.

6. ANALYSIS OF THE MOSSBAUER DATA IN TERMS OF BLUME-TJON FITS

In order to improve the method of analysis we decided to abandon the method of extracting linewidths directly, since it is not accurate enough. For the ^{57}Fe nucleus there are actually four values of ω_L, differing by about one order of magnitude. This is reflected in the asymmetric line broadening of the doublet at the higher temperatures (cf. fig. 3). In addition the line shapes become nonlorentzian for $\Gamma_\omega \approx \omega_L$, and the number of lines changes from two (the quadrupole doublet) to six or eight (the fully hyperfine split spectrum). This makes it impossible to determine $\Delta\Gamma$ directly in the region close to ω_L, which is just where crucial information about the flipping process can be obtained. Finally, there is quite a lot more potential information contained in the spectra on this process, notably in the form of the frequency (Γ_ω) dependence of the line-positions and the line-intensities.

In order to take advantage of the complete information hidden in the Mössbauer spectra, we have followed another approach, where we actually calculate **exactly** the resonance conditions (i.e. the total spectrum) for the Mössbauer nucleus in the presence of the nonlinear excitations. Since in the free-kink gas approximation the wall-motion causes stochastic spin-flips, this can be done in an elegant way. The resonance condition for the Mössbauer photon may be written as

$$W_{e,g}(\omega) \propto 2\Gamma_o^{-1}\ \mathrm{Re}\int_o^\infty dt\ \exp[(i\omega - \tfrac{1}{2}\Gamma_o)t] \sum_{\substack{e,g\\ e',g'}} \langle e'|H^-|g'\rangle\langle g|U^\dagger H^+ U|e\rangle \ . \tag{13}$$

Here $\hbar\omega$ is the energy of the ME photon, $|e\rangle$ and $|g\rangle$ are the nuclear excited and ground-state, respectively, and $U(t) = \exp(-i\mathcal{H}t)$ is the time-evolution operator for the total solid state, with hamiltonian $\mathcal{H}$, that enters in the multipole-operator $U^\dagger H^+ U$, in the Heisenberg representation. For $U^\dagger = U = 1$ (static limit), eq.(13) yields the superposition of lorentzian lines with FWHM Γ_o that are normally used to fit spectra. In general, calculation of the spectrum from eq.(13) will be fairly complex. For the present purpose, however, it may be greatly simplified. Since the dominant interactions between the ME nucleus and the solid state are the hyperfine interactions between the electrons and nucleus of the same atom, which are very small compared to the intra-nuclear interactions, the nuclear hamiltonian may be written as: $\mathcal{H} = \mathcal{H}_N + \mathcal{H}_{en} + \mathcal{H}_c$ with $\mathcal{H}_N$ the intra-nuclear hamiltonian, and $\mathcal{H}_{en}$ and $\mathcal{H}_c$ the perturbations due to the surrounding solid state. Here $\mathcal{H}_c$ represents the electric monopole interaction, which is of electrostatic origin and will be left aside in the discussion below. The time-dependence enters via the hamiltonian that describes the electronic-nuclear interaction $\mathcal{H}_{en}$, which is given by $\mathcal{H}_{en}=\mathcal{H}_Q+\mathcal{H}_M$. Here $\mathcal{H}_Q$ is the electric quadrupole interaction and $\mathcal{H}_M = -g\mu_n \vec{B}_{hf}(t)\vec{I}$ is the magnetic dipole interaction. The influence of the surrounding solid state is contained in the EFG tensor ($V_{zz}(t)$, $\eta(t)$) and the effective hyperfine field ($\vec{B}_{hf}(t)$). However, since the quadrupole interaction is of electric origin (and is time-even), it is not disturbed by magnetic domain wall-processes. This is not the case for $\vec{B}_{hf}$. In principle, three contributions to $\vec{B}_{hf}$ may be distinguished, namely the contributions due to the Fermi-contact interactions, due to the orbital moment and due to the dipolar interaction. All these are proportional to $\vec{S}$ or $\vec{L}$. Since the only effect relevant to the ME is the reversal of the total electronic spin upon the passage of a kink, i.e. the change of the sign of the components S_i and L_i, the time-dependent hyperfine field can be written as $\vec{B}_{hf}(t)=\vec{B}^0_{hf}f(t)$, where f(t) is a stochastic variable that jumps between ± 1 each time a kink passes.

Some time ago already, Blume and Tjon (BT) /34/ proposed an exact treatment for the elaboration of eq.(13) in case of a process of the type described in eq.(13). Extending their work, Clauser, and Shenoy et al. obtained an expression that is easily handled in a computer fitting procedure, and is given by

$$W_{e,g}(\omega) \propto \mathrm{Re}\sum_{\substack{e,g\\ e',g'}} (\langle e'|H^-|g'\rangle V)(V^{-1}\langle g|H^+|e\rangle)/(\Lambda - i\omega I) \quad . \tag{14}$$

Here I is the unit matrix and V, Λ are the eigen vectors and eigen values of a Liouville operator $\mathcal{H}^X$, defined by

$$\mathcal{H}^X = W + i(\mathcal{H}^X_Q F_Q + \mathcal{H}^X_M F_M) - \Gamma_o I \quad . \tag{15}$$

Here W is a matrix that contains all the physical information about the stochastic process and F is a diagonal matrix whose elements are the values assumed by the stochastic function f(t). These matrices are given by

$$W = \begin{pmatrix} -\Gamma_\omega & \Gamma_\omega \\ \Gamma_\omega & -\Gamma_\omega \end{pmatrix} \quad ; \quad F_Q = \begin{pmatrix} 1 & 0 \\ 0 & 1 \end{pmatrix} \quad , \quad F_M = \begin{pmatrix} 1 & 0 \\ 0 & -1 \end{pmatrix} \quad .$$

Thus the fact that $\vec{B}_{hf}$ jumps between two well-defined values permits the application of the BT relaxation model. Within this formalism the resonance conditions for the Mössbauer nucleus in the presence of stochastic domain-wall motion can be exactly calculated. This provides a way to test unambiguously whether soliton-type processes are indeed responsible for the relaxation effects observed in the spectra. By fitting eq.(14) to the experimental data the analysis becomes quite straightforward. In the fitting procedures the properties of the spectrum without relaxation effects are always determined separately at very low and very high temperatures, such that Γ_ω is outside the Mössbauer window set by the steady width Γ_o. This leaves Γ_ω as the only temperature-dependent adjustable parameter needed in fitting the computed spectra to the experimental ones and therefore this relaxation rate can be accurately studied as a function of different thermodynamic parameters (temperature, magnetic field, impurities). Some illustrative examples are discussed in the next section.

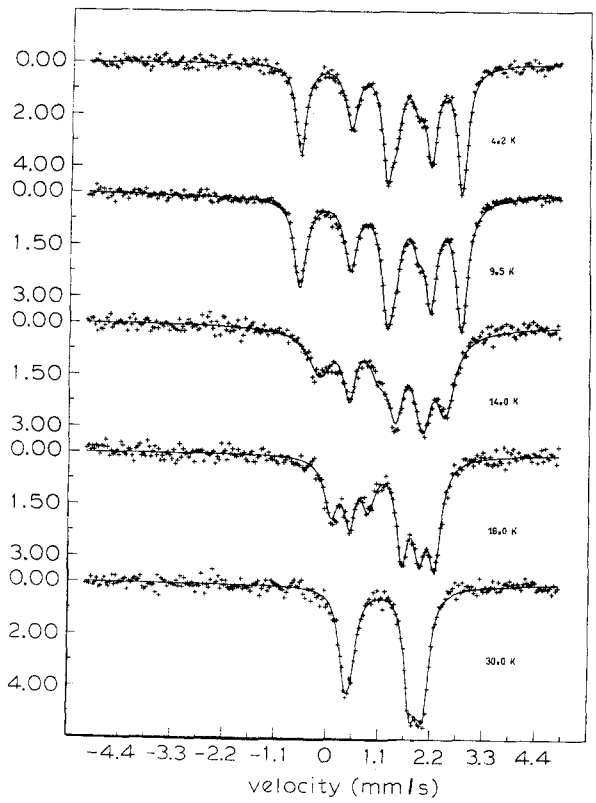

Fig. 4. Mössbauer spectra taken from $RbFeCl_3.2H_2O$ in an applied field B = 1.5 T. Solid lines represent the fits to the BT model.

7. EXPERIMENTAL RESULTS ANALYSED WITH THE BLUME-TJON MODEL

In fig. 4, some representative spectra are shown /4/ that were taken for $RbFeCl_3.2H_2O$ in a magnetic field B = 1.5 T applied along the c-axis. The solid lines represent the fits to the relaxation model described in the previous section and show how good the BT model may work in specific cases. We shall briefly discuss the phenomena that are seen in fig. 4. At the lowest temperature (T = 4.2 K) the lines are narrow (Γ = 0.26 mm/sec), but as the temperature is increased to 9.5 K the lines start to broaden, an indication that the flip rate Γ_ω is inside the Mössbauer window. Further increase of T causes still faster flipping and at T ≃ 30 K the lines are narrow again and Γ_ω is outside the window on the high-frequency side. The small splitting observed in the T = 30 K spectrum is due to the applied field. In fig. 5 another example is given /2/, namely $Fe_{1-c}Cd_cCl_2(NC_5H_5)_2$ with c = 0.47%. Again the solid lines are the fits to the relaxation model and the general features are comparable to those in fig. 4.

Results for Γ_ω are given in figs. 6 and 7. The data in fig. 6 concern $RbFeCl_3.2H_2O$, both in zero field and for B_c = 1.5 T. In zero field this system undergoes a transition towards 3-d long-range order at T_N = 11.96 K, but it has the special property that for $B_c > 1.24$ T the 3-d order is completely absent, even at the lowest temperatures /37/. This arises from the fact that in an antiferromagnet T_c is reduced to zero by a sufficiently strong field. The value of T_N is indicated by the arrow in fig. 6. The data in fig. 7 are for $Fe_{1-c}Cd_cCl_2(NC_5H_5)_2$. Dilution of $FeCl_2(NC_5H_5)_2$ with small amounts of nonmagnetic Cd characteristically reduces the magnetic correlation length ($\xi^{1d}_{max} \propto c^{-1}$), whereas the general behaviour of the magnetic chain is not altered. Since $k_B T_c \simeq \xi^{1d} J' |S^2|$, with J' the interchain

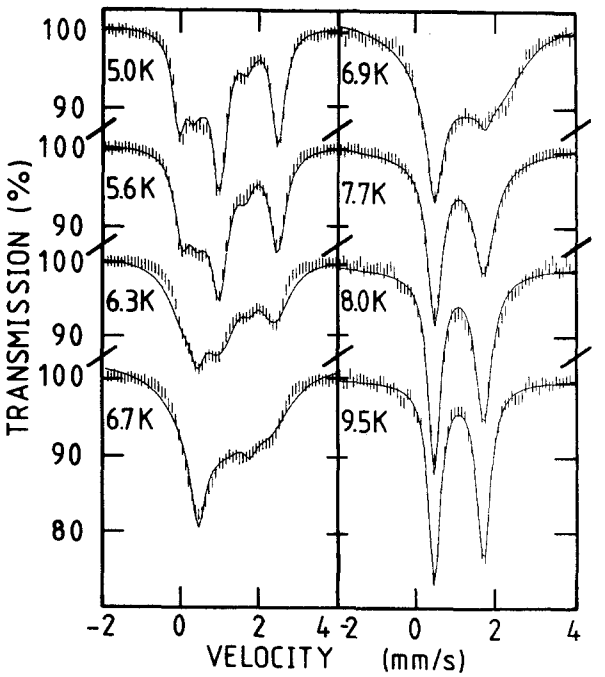

Fig. 5. Mössbauer spectra taken from $Fe_{1-c}Cd_c(NC_5H_5)_2$ with c=0.47%. Solid lines represent the fits to the BT model.

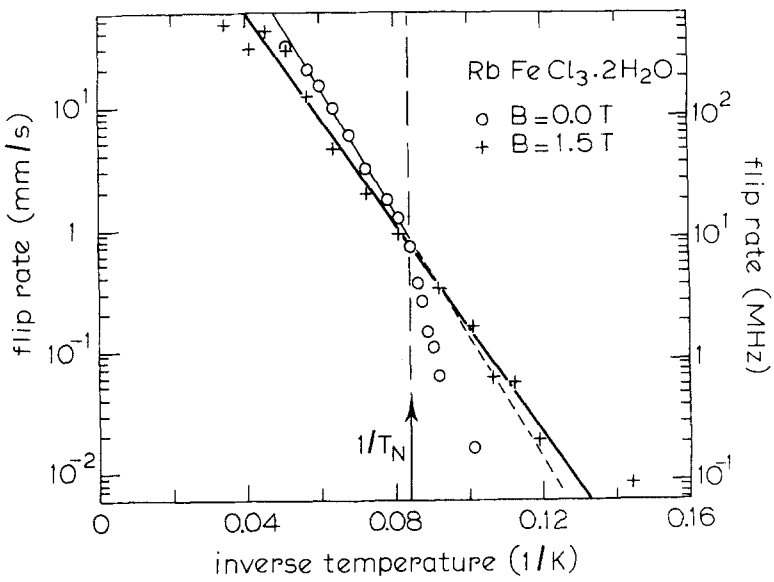

Fig. 6 Results from the analysis with the BT model: flip rate versus inverse temperature for $RbFeCl_3.2H_2O$, in zero field and in an applied field of B = 1.5 T.

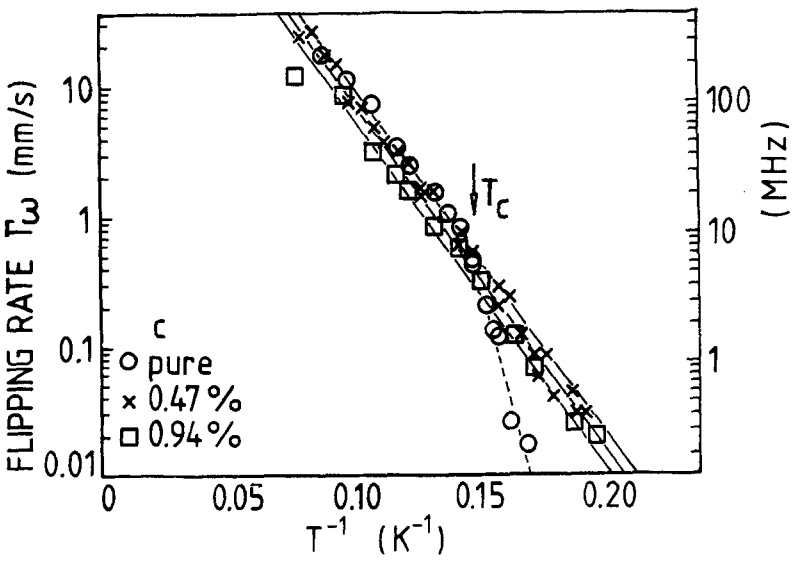

Fig. 7. Flip rate versus inverse temperature for the $Fe_{1-c}Cd_cCl_2(NC_5H_5)_2$ samples, pure (c=0) and with small amounts of cadmium (c=0.47%) and c=0.94%).

exchange interaction, a decrease of ξ^{1d} reduces T_c and thus has the same effect as application of a field B_c in the case of $RbFeCl_3.2H_2O$: the 3-d order is suppressed and T_c becomes lower with respect to the value in the pure compound (T_c = 6.6 K; as indicated by the arrow in fig. 7). Such tricks enable a check on the blocking effect of 3-d order on the wall-dynamics, both in the ferromagnetic and in the antiferromagnetic examples. It appears that the effects of the 3-d order are comparable to those observed in $Fe(N_2H_5)_2(SO_4)_2$ (fig. 3). In $RbFeCl_3.2H_2O$ with $B_c = 0$, Γ_ω varies exponentially with T^{-1} but drops sharply at T_N and rapidly falls outside the Mössbauer window (fig. 6). The same holds for **pure** $FeCl_2(NC_5H_5)_2$. However, when T_c is suppressed either by putting a field on the system or by diluting with nonmagnetic ions, Γ_ω behaves exponentially down to the lowest frequencies that may be observed with the Mössbauer nucleus. When the system is 3-d ordered the kinks should become frozen and accordingly no dynamics is observed.

In the $Fe_{1-c}M_cCl_2(NC_5H_5)_2$ systems the coupling between the chain-segments on both sides of an impurity should remain present if a magnetic impurity ion is taken for M instead of nonmagnetic Cd. This is confirmed by the data /38/ in fig. 8, where results for Γ_ω versus T^{-1} with small amounts of magnetic impurities (Ni, Mn, Co, Cu) are shown. The data for the pure compound are included for comparison. The T_c-values correspond to those deduced from χ-measurements. They differ slightly for each kind of magnetic impurity, as expected, since they obviously will depend on the strength of the interactions between the impurity moment and the neighbouring Fe^{2+} ion. An interesting point is that both dilution experiments, with magnetic as well as nonmagnetic impurities, show no variation in the slope of the ex-

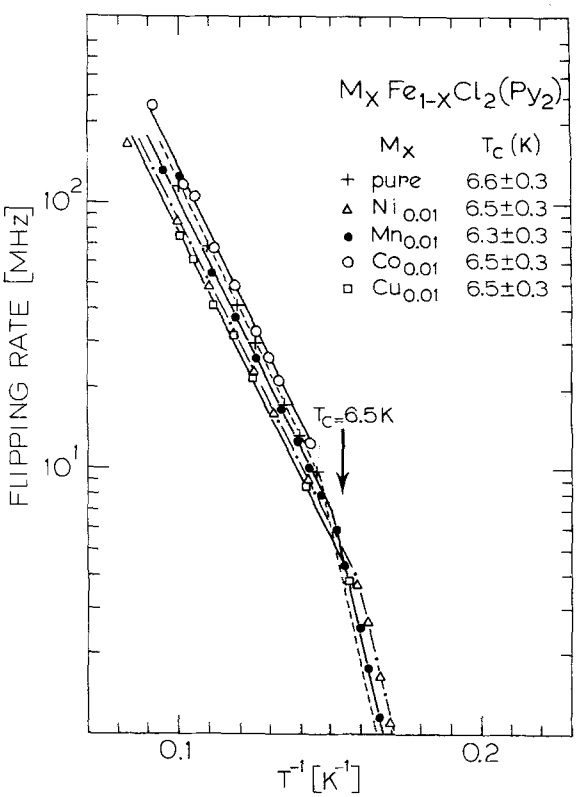

Fig. 8.
Fliprate versus inverse temperature for the $Fe_{0.99}M_{0.01}Cl_2(NC_5H_5)_2$ samples. The results for the pure Fe sample are included for comparison.

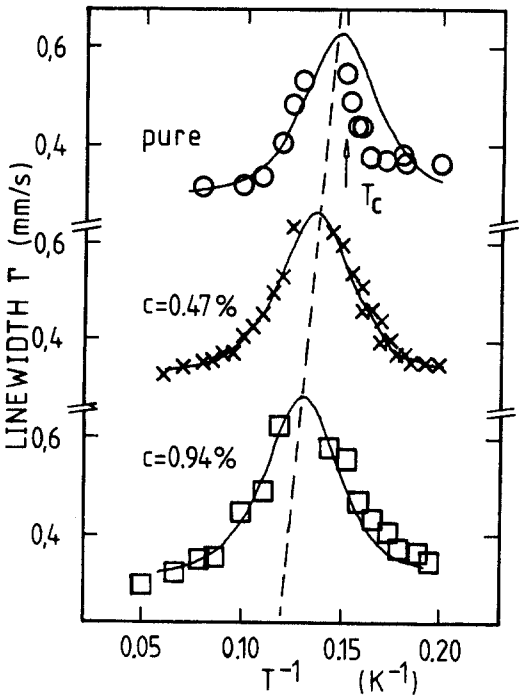

Fig. 9. Linewidth versus inverse temperature for the pure $FeCl_2(NC_5H_5)_2$ and the two cadmium-diluted samples. The spectra were analysed with a superposition of lorentzian lines. Solid lines represent the calculated behaviour of the free-kink gas model with E_s = 60 K. The dashed line is a guide to the eye.

perimental curves. Only a slight shift along the temperature axis occurs. This is also seen in fig. 9, where we show the results of the method of analysis of the linewidth for the Cd-diluted compounds and the pure compounds. The most striking effect in this picture is the removal of T_c in the Cd-containing compounds, revealing the full symmetric excess-linewidth behaviour. The shift towards higher temperatures upon dilution is indicated by the dashed line in this figure.

The exponential variation of Γ_ω with T^{-1} is in good qualitative agreement with the predictions from the free-kink gas model. As was explained in section 3, one has $\Gamma_\omega = n_s v_s$ and thus $\Gamma_\omega \propto \exp(-E_s/k_BT)$. However, if one compares the experimental values for E_s with the theoretical ones, one finds an important difference. Both are mentioned in table I for all compounds. It appears that the exponents observed are all of the order of $2E_s$. It is as if only **wall-pair** excitations (which have an excitation energy of $2E_s$) are seen in the Mössbauer spectrum, in contrast to what the theory predicts. It may be noted that the prediction is not only from free-kink gas theory but also follows from the exact expression for the correlation length of the Ising chain (i.e. hamiltonian (1) with $\varepsilon = 0$), $\xi^{1d} = -[\ln(\tanh(J_x/2k_BT))]^{-1}$, which may be approximated at low temperatures ($T \ll J_x/k_B$) by $\xi^{1d} = \frac{1}{2}\exp(J_x/k_BT)$. Since $E_s \to J_x$ for $\varepsilon \to 0$ (eq.(5)), this is in agreement with the free-kink gas model, where one has /32/ $\xi^{1d} = \frac{1}{2} n_s^{-1} \propto \exp(E_s/k_BT)$. Furthermore we remark that the same functional dependence of ξ^{1d} was obtained in transfer-matrix /32/ and finite-chain calculations /39/. Essentially, the temperature dependence of the correlation length in Ising-type chains is thus given by $\xi^{1d} \propto \exp(E_s/k_BT)$, with E_s the excitation energy of a **single kink**. This has been verified in quite a number of experiments on domain walls in magnetic chains, notably the neutron scattering studies on TMMC /40/, and on $CsCoCl_3$ /41,42/ and $CsCoBr_3$ /43/. A recent study by two of us on the phase diagrams of quasi 1-d antifer-

romagnets /44/ revealed the same dependence of ξ^{1d} on E_s. We are therefore confident that the single-kink density $n_s \propto 1/\xi^{1d}$ is indeed given by $n_s \propto \exp(-E_s/k_BT)$.

However, the Mössbauer experiments are quite conclusive as well. They yield $\Gamma_\omega \propto \exp(-2E_s/k_BT)$, where E_s is calculated from exchange and anisotropy constants determined in separate experiments (χ, specific heat). A possible way-out of this dilemma would be that the Γ_ω seen by the ME probe corresponds to the excitation of **wall-pairs**, the actual single-kink density being very much higher. For example, the typical experimental value $\Gamma_\omega \simeq 10$ MHz yields a (very low) density $n_s = 2.10^{-6}$ for $RbFeCl_3.2H_2O$ if the relationship $\Gamma_\omega = n_s v_s$ is assumed. On the other hand a more reasonable value of $n_s = 4.10^{-2}$ is obtained when at the appropriate temperature n_s is calculated according to eq.(9), using the parameters in table I for this compound.

We are presently engaged in trying to solve this puzzle. One possibility would be the existence of a soliton-lattice structure, static on Mössbauer time scales, with kinks separated at regular average spacings due to repulsive interactions between them. The average density of single kinks should be dictated by entropy considerations. The additional wall-pair excitations would temporarily disrupt this structure, which would then be the effect seen by the ME probe.

Acknowledgements

We are much indebted to J. Reedijk of the "Werkgroep voor Fundamenteel Materialenonderzoek (WFMO)" of the State University of Leiden and to W.J.M. de Jonge of the Technical University of Eindhoven for providing the samples. Also H.Th. Le Fever is gratefully acknowledged for putting his data on the $Fe(N_2H_5)_2(SO_4)_2$ compound at our disposal for reanalysis. We have much benefitted by the cooperation with C.E. Johnson and M.F. Thomas of the University of Liverpool in the experiments on $RbFeCl_3.2H_2O$. This work is part of the research program of the Stichting voor Fundamenteel Onderzoek der Materie (Foundation for Fundamental Research on Matter) and was made possible by financial support from the Nederlandse Organisatie voor Zuiver Wetenschappelijk Onderzoek (Netherlands Organization for the Advancement of Pure Research).

References

/1/ R.C. Thiel, H. de Graaf, L.J. de Jongh, Phys. Rev. Letters 47(1981)1415.
/2/ H.J.M. de Groot, L.J. de Jongh, R.C. Thiel and J. Reedijk, Phys. Rev. B30(1984)4041.
/3/ H.J.M. de Groot, R.C. Thiel and L.J. de Jongh, in Magnetic Excitations and Fluctuations, eds. S.W. Lovesey, U. Balucani, F. Borsa and V. Tognetti, (Springer, Berlin, 1984)p.21.
/4/ H.H.A. Smit, H.J.M. de Groot, R.C. Thiel, L.J. de Jongh, C.E. Johnson and M.F. Thomas, Sol. St. Comm. 53(1985)573.
/5/ See e.g. L.J. de Jongh, J. Appl. Phys. 53(1982)8018; and references cited therein.
/6/ L.W. Levinson and M. Luban, Phys. Rev. 172(1968)268.
/7/ A.D. Bruce, in Solitons and Condensed Matter Physics, eds. A.R. Bishop and T. Schneider, (Springer, Berlin, 1978)p.116.
/8/ F.C. Frank and J.H. van der Merwe, Proc. Roy. Soc. London 198(1949)205; for a recent review, see e.g. J. Villain, in Ordering in Strongly Fluctuating Condensed Matter Systems, ed. T. Riste, (Plenum, New York, 1980)p.221.
/9/ A.S. Davydov, J. Theor. Biology 38(1973)559.
/10/ W.P. Su, J.R. Schrieffer and A.J. Heeger, Phys. Rev. Letters

42(1979)1698.
/11/ G. Grüner and A. Zettl, Phys. Repts. 119(1985)117.
/12/ See e.g. V.J. Emery, in Highly Conducting One-Dimensional Solids, eds. J.T. Devreese, R.P. Evrard and V.E. van Doren, (Plenum, New York, 1979)p.286.
/13/ V.L. Pokrovski and A.L. Talapov, Zh. Eksp. Teor. Fiz. 78(1980)269 (JETP 51 (1980)1).
/14/ D.G. Rancourt, S.R. Julian and J.M. Daniels, J. Magn. Magn. Mat. 51(1985).
/15/ H.Th. Lefever, R.C. Thiel, W.J. Huiskamp and W.J.M. de Jonge, Physica 111B(1981)190.
/16/ K. Kopinga, Q.A.G. van Vlimmeren, A.L.M. Bongaarts and W.J.M. de Jonge, Physica 86-88 B+C(1977)671; Q.A.G. van Vlimmeren, thesis.
/17/ G.J. Long, D.L. Whitney and J.E. Kennedy, Inorg. Chem. 10(1971)1406; P.C.M. Gubbens, W. Ras, A.M. van der Kraan and J. Reedijk, in Proceedings of the International Conference on Applications of the Mössbauer Effect-1981, Jaipur (The Indian National Science Academy, New Delhi, 1982).
/18/ B.F. Little and G.J. Long, Inorg. Chem. 17(1978)3401.
/19/ W.M. Reiff, H. Wong, R.B. Frankel and S. Foner, Inorg. Chem. 16(1977)1036.
/20/ See also: A. Nieuwpoort and J. Reedijk, Inorg. Chim. Acta 7(1973)323.
/21/ U. Enz, Helvetica Physica Acta 37(1964)245.
/22/ H.J. Mikeska, J. Phys. C13(1980)2913; H.J. Mikeska, J. Appl. Phys. 52(1981)1950.
/23/ J. Villain, Physica 79B(1975)1.
/24/ C. Kittel, Introduction to Solid State Physics, (Wiley, New York, 1953)p.488.
/25/ For a review see e.g. A.R. Bishop, J.A. Krumhansl and S.E. Trullinger, Physica D1(1980)1.
/26/ C. Etrich and H.J. Mikeska, J. Phys. C16(1983)4889.
/27/ E. Magyari and H. Thomas, Phys. Rev. Letters 51(1983)54.
/28/ N. Ishimura and H. Shiba, Progr. Theor. Phys. 63(1980)743.
/29/ See also: J.B. Torrance and M. Tinkham, Phys. Rev. 187(1968)587.
/30/ L.D. Landau and E.M. Lifshitz, in Statistical Physics (Pergamon, Oxford, 1958)p.482.
/31/ J.F. Currie, J.A. Krumhansl, A.R. Bishop and S.E. Trullinger, Phys. Rev. B22(1980)477.
/32/ K. Maki, in Progress in Low Temperature Physics, ed. D.F. Brewer, (North-Holland, Amsterdam, 1981)Vol. VIII.
/33/ F. Borsa, Phys. Letters 80A(1980)309.
/34/ M. Blume and J.A. Tjon, Phys. Rev. 165(1968)446; M. Blume, Phys. Rev. 174(1968)351.
/35/ M.J. Clauser, Phys. Rev. B3(1971)583.
/36/ K. Shenoy and B. Dunlap, in Proc. Int. Conf. on Mössb. Spectr. (Cracow 1975)p.275.
/37/ J.A.J. Basten, Q.A.G. van Vlimmeren and W.J.M. de Jonge, Phys. Rev. B18(1978)2179.
/38/ M. ElMassalami, to be published.
/39/ J.D. Johnson and J.C. Bonner, Phys. Rev. B22(1980)251.
/40/ J.P. Boucher, L.P. Regnault, J. Rossat-Mignod, J.P. Renard, J. Bouillot and W.G. Stirling, J. Appl. Phys. 52(1981)1956.
/41/ H. Yoshizawa, K. Hirakawa, S.K. Satija and G. Shirane, Phys. Rev. B23(1981)2298.
/42/ J.P. Boucher, L.P. Regnault, J. Rossat-Mignod, Y. Henry, J. Bouillot and W.G. Stirling, Phys. Rev. B31(1985)3015.
/43/ S.E. Nagler, W.J.L. Buyers, R.L. Armstrong nd B. Briat, Phys. Rev. B28(1983)3873.
/44/ L.J. de Jongh and H.J.M. de Groot, Sol. St. Comm. 53(1985)731.